Models of membrane electrostatics

Kevin Cahill[*]

Biophysics Group, Department of Physics & Astronomy, University of New Mexico, Albuquerque, New Mexico 87131, USA and
Physics Department, Fudan University, Shanghai 200433, China

Formulas are derived for the electrostatic potential of a charge in or near a membrane modeled as one or more dielectric slabs lying between two semi-infinite dielectrics. One can use these formulas in Monte Carlo codes to compute the distribution of ions near cell membranes more accurately than by using Poisson-Boltzmann theory or its linearized version. Here I use them to discuss the electric field of a uniformly charged membrane, the image charges of an ion, the distribution of salt ions near a charged membrane, the energy of a zwitterion near a lipid slab, and the effect of including the phosphate head groups as thin layers of high electric permittivity.

I. CELL MEMBRANES

The plasma membrane of an animal cell and the membranes of the endoplasmic reticulum, the Golgi apparatus, the endosomes, and other membrane-enclosed organelles are lipid bilayers about 5 nm thick studded with proteins. The lipid constituents are mainly phospholipids, sterols, and glycolipids.

Of the four main phospholipids in membranes, three—phosphatidylethanolamine (PE), phosphatidylcholine (PC), and sphingomyelin (SM)—are neutral, and one, phosphatidylserine (PS), is negatively charged. In a living cell, PE and PS are mostly in the cytosolic layer of the plasma membrane; PC and SM are mostly in the outer layer [1]; and the electrostatic potential of the cytosol is 20 to 120 mV lower than that of the extracellular environment.

After pioneering work by Gouy, Chapman, and Wagner [2] and Onsager and Samaras [3], many scientists have studied the electrical properties of cell membranes [4,5]. This paper presents the exact electrostatic potential due to a charge in or near a membrane in the continuum limit in which the membrane is taken to be one or more dielectric slabs lying between two different infinite dielectric media. Because of the superposition principle, this monopole potential also gives the multipole potential due to any array of charges in or near a membrane.

One can use these formulas to simulate the interactions of ions with other ions and with fixed charges near membranes while modeling water and other neutral molecules as bulk media. For instance, one can use them in Monte Carlo simulations to compute the behavior of salt ions and protons in water near neutral or charged membranes even in the presence of fixed charges of arbitrary geometry. This method is more accurate than the Poisson-Boltzmann mean-field approximation and much more accurate than its linearized version [6]. These formulas also provide a context for and a check on all-atom computer simulations [6,7].

As early as 1924, Wagner [2] noted that an ion in water near a lipid slab induces image charges that repel the ion. No mean-field theory can describe this simple effect, but work-arounds are available for the Poisson-Boltzmann theory [5].

Formulas for the electrostatic potential of a charge in or near a cell membrane modeled as a single slab are derived in Sec. II. As pedagogical illustrations of their utility, I use them to compute the electric field of a charged membrane in Sec. III and the response of bound charge to an ion in Sec. IV. In Sec. V, I use them to simulate the distribution of salt ions near a charged membrane. I discuss the Debye layer in Sec. VI and the energy of a zwitterion near a lipid slab in Sec. VII. In Sec. VIII, I calculate the potential of a charge near a membrane modeled as several dielectric layers of different permittivities between two different semi-infinite dielectrics. I use this analysis in Sec. IX to model a phospholipid bilayer as a lipid layer bounded by two layers of head groups of high electric permittivity. The phosphate head groups cause the membrane to attract rather than to repel ions. I summarize the paper in Sec. X.

II. THE POTENTIAL OF A CHARGE IN OR NEAR A LIPID BILAYER

In electrostatic problems, Maxwell's equations reduce to Gauss's law $\nabla \cdot \mathbf{D} = \rho_f$, which relates the divergence of the electric displacement $\mathbf{D}$ to the free-charge density ρ_f (not including the polarization of the medium), and the static form of Faraday's law $\nabla \times \mathbf{E} = 0$, which implies that the electric field $\mathbf{E}$ is the gradient of an electrostatic potential $\mathbf{E} = -\nabla V$.

Across an interface with normal vector $\hat{\mathbf{n}}$ between two dielectrics, the tangential component of the electric field is continuous,

$$\hat{\mathbf{n}} \times (\mathbf{E}_2 - \mathbf{E}_1) = 0, \tag{1}$$

while the normal component of the electric displacement jumps by the surface density σ of free charge:

$$\hat{\mathbf{n}} \cdot (\mathbf{D}_2 - \mathbf{D}_1) = \sigma. \tag{2}$$

In a linear dielectric, the electric displacement $\boldsymbol{D}$ is the electric field scaled by the permittivity ϵ of the material $\boldsymbol{D} = \epsilon \, \boldsymbol{E}$.

The lipid bilayer is taken to be flat, extending to infinity in the x-y plane, and of a thickness $t \approx 5$ nm. The interface between the extracellular salty water and the lipid bilayer is at $z = 0$. The permittivity ϵ_ℓ of the lipid bilayer is about twice that of the vacuum $\epsilon_\ell \approx 2\epsilon_0$; those of the extracellular environment ϵ_w and of the cytosol ϵ_c are about 80 times ϵ_0.

———————
[*]cahill@unm.edu

The potential of a charge q at a point $(0,0,h)$ on the z axis is cylindrically symmetric, and so Bessel functions are useful here. In cylindrical coordinates with $\rho = \sqrt{x^2 + y^2}$, the functions $J_n(k\rho)\, e^{in\phi}\, e^{\pm kz}$ form a complete set of solutions of Laplace's equation, but due to the azimuthal symmetry, we only need the $n = 0$ functions $J_0(k\rho)\, e^{\pm kz}$. We will use them and the relation [8]

$$\frac{1}{\sqrt{\rho^2 + (z-h)^2}} = \int_0^\infty dk\, J_0(k\rho)\, e^{-k|z-h|} \qquad (3)$$

to represent the potential of point charge at $(0,0,h)$.

If the charge q is at $(0,0,h)$ in the water above the membrane ($h > 0$), then we may write the potentials in the extracellular water V_w^w, in the lipid membrane V_ℓ^w, and in the cytosol V_c^w as

$$V_w^w(\rho,z) = \int_0^\infty dk\, J_0(k\rho)\left[\frac{q}{4\pi\epsilon_w} e^{-k|z-h|} + u(k)\, e^{-kz}\right],$$

$$V_\ell^w(\rho,z) = \int_0^\infty dk\, J_0(k\rho)[m(k)\, e^{kz} + f(k)\, e^{-kz}],$$

$$V_c^w(\rho,z) = \int_0^\infty dk\, J_0(k\rho)\, d(k)\, e^{kz}. \qquad (4)$$

Imposing the constraints (1) and (2), writing $u(k)$ as u, $m(k)$ as m, and so forth, and setting $\beta \equiv qe^{-kh}/4\pi\epsilon_w$ and $y = e^{2kt}$, we get the four equations

$$
\begin{aligned}
m + f - u &= \beta, \\
\epsilon_\ell m - \epsilon_\ell f + \epsilon_w u &= \epsilon_w \beta, \\
\epsilon_\ell m - \epsilon_\ell y f - \epsilon_c d &= 0, \\
m + y f - d &= 0.
\end{aligned}
\qquad (5)
$$

In terms of the abbreviations

$$\epsilon_{w\ell} = \frac{1}{2}(\epsilon_w + \epsilon_\ell) \quad \text{and} \quad \epsilon_{c\ell} = \frac{1}{2}(\epsilon_c + \epsilon_\ell),$$

$$p = \frac{\epsilon_w - \epsilon_\ell}{\epsilon_w + \epsilon_\ell} \quad \text{and} \quad p' = \frac{\epsilon_c - \epsilon_\ell}{\epsilon_c + \epsilon_\ell}, \qquad (6)$$

their solutions are

$$u(k) = \beta\, \frac{p - p'/y}{1 - pp'/y},$$

$$m(k) = \beta\, \frac{\epsilon_w}{\epsilon_{w\ell}}\, \frac{1}{1 - pp'/y},$$

$$f(k) = -\beta\, \frac{\epsilon_w}{\epsilon_{w\ell}}\, \frac{p'/y}{1 - pp'/y}, \qquad (7)$$

$$d(k) = \beta\, \frac{\epsilon_w \epsilon_\ell}{\epsilon_{w\ell}\epsilon_{c\ell}}\, \frac{1}{1 - pp'/y}.$$

Inserting these solutions into the Bessel expansions (4) for the potentials, expanding their denominators

$$\frac{1}{1 - pp'/y} = \sum_0^\infty (pp')^n\, e^{-2nkt}, \qquad (8)$$

and using the integral (3), we find that the potential $V_w^w(\rho,z)$ in the extracellular water due to a charge q at $(0,0,h)$ in that

water is

$$
\begin{aligned}
V_w^w(\rho,z) = \frac{q}{4\pi\epsilon_w}\Bigg[&\frac{1}{r} + \frac{p}{\sqrt{\rho^2 + (z+h)^2}} \\
&- p'(1 - p^2)\sum_{n=1}^\infty \frac{(pp')^{n-1}}{\sqrt{\rho^2 + (z + 2nt + h)^2}} \Bigg],
\end{aligned}
$$
$$(9)$$

in which $r = \sqrt{\rho^2 + (z-h)^2}$ is the distance to the charge q, and $\sqrt{\rho^2 + (z+h)^2}$ is the distance to the principal image charge pq. Similarly, the potential V_ℓ^w in the lipid bilayer is

$$
\begin{aligned}
V_\ell^w(\rho,z) = \frac{q}{4\pi\epsilon_{w\ell}}\sum_{n=0}^\infty (pp')^n \Bigg\{ &\frac{1}{\sqrt{\rho^2 + (z - 2nt - h)^2}} \\
&- \frac{p'}{\sqrt{\rho^2 + [z + 2(n+1)t + h]^2}} \Bigg\},
\end{aligned}
\qquad (10)
$$

and the potential V_c^w in the cytosol is

$$V_c^w(\rho,z) = \frac{q\,\epsilon_\ell}{4\pi\epsilon_{w\ell}\epsilon_{c\ell}}\sum_{n=0}^\infty \frac{(pp')^n}{\sqrt{\rho^2 + (z - 2nt - h)^2}}. \qquad (11)$$

If the charge q is in the lipid bilayer at $(0,0,h)$ where $(-t < h < 0)$, then the Bessel representations of the potentials are

$$V_w^\ell(\rho,z) = \int_0^\infty dk\, J_0(k\rho)\, u(k)\, e^{-kz},$$

$$
\begin{aligned}
V_\ell^\ell(\rho,z) = \int_0^\infty dk\, J_0(k\rho)\Bigg[&\frac{q}{4\pi\epsilon_\ell} e^{-k|z-h|} \\
&+ m(k)\, e^{kz} + f(k)\, e^{-kz} \Bigg],
\end{aligned}
\qquad (12)
$$

$$V_c^\ell(\rho,z) = \int_0^\infty dk\, J_0(k\rho)\, d(k)\, e^{kz}.$$

With $\gamma = qe^{kh}/4\pi\epsilon_\ell$ and $x = e^{-2kh}$, the Maxwell constraints (1) and (2) give us the equations

$$
\begin{aligned}
u - m - f &= \gamma, \\
\epsilon_w u + \epsilon_\ell m - \epsilon_\ell f &= \epsilon_\ell \gamma, \\
d - m - y f &= x\gamma, \\
\epsilon_c d - \epsilon_\ell m - \epsilon_\ell y f &= \epsilon_\ell x\gamma,
\end{aligned}
\qquad (13)
$$

whose solutions are

$$u(k) = \frac{\epsilon_\ell \beta}{\epsilon_{w\ell}}\, \frac{1 - p'x/y}{1 - pp'/y},$$

$$m(k) = -p\beta\, \frac{1 - p'x/y}{1 - pp'/y},$$

$$f(k) = -\frac{p'\beta}{y}\, \frac{x - p}{1 - pp'/y}, \qquad (14)$$

$$d(k) = \frac{\epsilon_\ell \beta}{\epsilon_{c\ell}}\, \frac{x - p}{1 - pp'/y}.$$

After putting these solutions into the Bessel expansions (12) and using the integral (3) and the denominator sum (8), one finds that the potential V_w^ℓ in the extracellular water due

to a charge q at $(0,0,h)$ in the lipid bilayer is

$$V_w^\ell(\rho,z) = \frac{q}{4\pi\epsilon_{w\ell}} \left\{ \sum_{n=0}^\infty \frac{(pp')^n}{\sqrt{\rho^2 + (z + 2nt - h)^2}} \right.$$
$$\left. - \sum_{n=0}^\infty \frac{p'(pp')^n}{\sqrt{\rho^2 + [z + 2(n+1)t + h]^2}} \right\}. \quad (15)$$

The potential V_ℓ^ℓ in the lipid bilayer is

$$V_\ell^\ell(\rho,z) = \frac{q}{4\pi\epsilon_\ell} \left\{ \sum_{n=-\infty}^\infty \frac{(pp')^{|n|}}{\sqrt{\rho^2 + (z - 2nt - h)^2}} \right.$$
$$- \sum_{n=0}^\infty \frac{p(pp')^n}{\sqrt{\rho^2 + (z - 2nt + h)^2}}$$
$$\left. - \sum_{n=0}^\infty \frac{p'(pp')^n}{\sqrt{\rho^2 + [z + 2(n+1)t + h]^2}} \right\}, \quad (16)$$

and that V_c^ℓ in the cytosol is

$$V_c^\ell(\rho,z) = \frac{q}{4\pi\epsilon_{c\ell}} \left[\sum_{n=0}^\infty \frac{(pp')^n}{\sqrt{\rho^2 + (z - 2nt - h)^2}} \right.$$
$$\left. - \frac{p(pp')^n}{\sqrt{\rho^2 + (z - 2nt + h)^2}} \right]. \quad (17)$$

Finally and somewhat redundantly, we turn to the case of a charge q in the cytosol at $(0,0,h)$ with $h < -t$. Now the Bessel expansions of the potentials are

$$V_w^c(\rho,z) = \int_0^\infty dk\, J_0(k\rho)\, u(k)\, e^{-kz},$$
$$V_\ell^c(\rho,z) = \int_0^\infty dk\, J_0(k\rho) \left[m(k)\, e^{kz} + f(k)\, e^{-kz} \right], \quad (18)$$
$$V_c^c(\rho,z) = \int_0^\infty dk\, J_0(k\rho) \left[\frac{q}{4\pi\epsilon_w} e^{-k|z-h|} + d(k)\, e^{kz} \right].$$

The continuity conditions (1) and (2) give us the four equations

$$u - m - f = 0,$$
$$\epsilon_w u + \epsilon_\ell m - \epsilon_\ell f = 0,$$
$$d - m - yf = -\beta y, \quad (19)$$
$$\epsilon_c d - \epsilon_\ell m + \epsilon_\ell yf = \beta cy,$$

whose solutions are

$$u(k) = \frac{\epsilon_\ell \epsilon_c}{\epsilon_{w\ell} \epsilon_{c\ell}} \frac{\beta}{1 - pp'/y},$$
$$m(k) = -\frac{\epsilon_c}{\epsilon_{c\ell}} \frac{p\beta}{1 - pp'/y},$$
$$f(k) = \frac{\epsilon_c}{\epsilon_{c\ell}} \frac{\beta}{1 - pp'/y}, \quad (20)$$
$$d(k) = \beta \frac{p'y - p}{1 - pp'/y}.$$

Thus, using (3) and (8) in (18), we find that the potential V_w^c in the extracellular water due to a charge q at $(0,0,h)$ in

the cytosol is

$$V_w^c(\rho,z) = \frac{q\,\epsilon_\ell}{4\pi\,\epsilon_{w\ell}\,\epsilon_{c\ell}} \sum_{n=0}^\infty \frac{(pp')^n}{\sqrt{\rho^2 + (z + 2nt - h)^2}}. \quad (21)$$

The potential V_ℓ^c in the lipid bilayer is

$$V_\ell^c(\rho,z) = \frac{q}{4\pi\,\epsilon_{c\ell}} \left[\sum_{n=0}^\infty \frac{(pp')^n}{\sqrt{\rho^2 + (z - h + 2nt)^2}} \right.$$
$$\left. - p \sum_{n=0}^\infty \frac{(pp')^n}{\sqrt{\rho^2 + (z + h - 2nt)^2}} \right]. \quad (22)$$

The potential V_c^c in the cytosol is

$$V_c^c(\rho,z) = \frac{q}{4\pi\epsilon_c} \left[\frac{1}{r} + \frac{p'}{\sqrt{\rho^2 + (z + h + 2t)^2}} \right.$$
$$\left. - p(1 - p'^2) \sum_{n=0}^\infty \frac{(pp')^n}{\sqrt{\rho^2 + (z - 2nt + h)^2}} \right] \quad (23)$$

in which r is the distance to the charge and $\sqrt{\rho^2 + (z + h + 2t)^2}$ is the distance to the principal image charge $p'q$.

Inasmuch as $1 - p^2 = \epsilon_w \epsilon_\ell / \epsilon_{w\ell}^2$, the series (9)–(11) for the potentials $V_\ell^w(\rho,z)$, $V_w^w(\rho,z)$, and $V_c^w(\rho,z)$ agree with those derived by the method of image charges [9]. The first eight terms of the infinite series (9)–(11), (15)—(17), and (21)—(23) give the potentials to within 1%. They are fast.

The first 1000 terms of the series (9), (10), and (11) for the potentials $V_\ell^w(\rho,z)$, $V_w^w(\rho,z)$, and $V_c^w(\rho,z)$ (right curve, blue) and (21), (22), and (23) for the potentials $V_\ell^c(\rho,z)$, $V_w^c(\rho,z)$, and $V_c^c(\rho,z)$ (left curve, red) are plotted in Fig. 1 (V) for $\rho = 1$ nm as a function of the height z (nm) above the phospholipid bilayer for a unit charge $q = |e|$ in the extracellular medium at $(\rho,z) = (0,1)$ nm (right curve, blue) and in the cytosol at $(\rho,z) = (0,-6)$ nm (left curve, red). The errors due to the truncation of these series at 1000 terms are less than 1 part in 10^{15}.

The first 1000 terms of the series (15), (16), and (17) for the potentials $V_\ell^\ell(\rho,z)$, $V_w^\ell(\rho,z)$, and $V_c^\ell(\rho,z)$ are plotted in Fig. 2 (V) for $\rho = 1$ nm as a function of the height z (nm) above the phospholipid bilayer for a unit charge $q = |e|$ in the bilayer at $(\rho,z) = (0,-4.5)$ (left curve, blue), $(0,-2.5)$ (middle curve, magenta), and $(0,-0.5)$ nm (right curve, red). The lipid bilayer extends from $z = -5$ to $z = 0$ nm and is bounded by thin (black) vertical lines in Figs. 1 and 2. The cytosol lies below $z = -5$ nm. The relative permittivities were taken to be $\epsilon_w = \epsilon_c = 80$ and $\epsilon_\ell = 2$.

Figures 1 and 2 show that the potentials fall off sharply as they cross the lipid bilayer. The reason for this effect is a buildup of bound charge in the water near the lipid bilayer due to the high electric permittivities of the extracellular environment ϵ_w and of the cytosol ϵ_c.

In Secs. VIII and IX, I extend this derivation to the case of several dielectric slabs. This generalization allows us to add
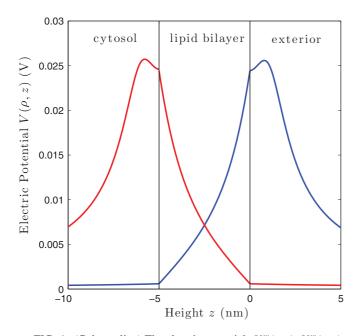
FIG. 1. (Color online) The electric potentials $V_w^w(\rho,z)$, $V_\ell^w(\rho,z)$, and $V_c^w(\rho,z)$ [(9), (10), and (11)] and $V_w^c(\rho,z)$, $V_\ell^c(\rho,z)$, and $V_c^c(\rho,z)$ [(21), (22), and (23)] are plotted (V) for $\rho = 1$ as a function of the height z above the phospholipid bilayer for a unit charge $q = |e|$ in the extracellular salty water at $(0,1)$ (right curve, blue) and in the cytosol at $(\rho,z) = (0,-6)$ (left curve, red). The lipid bilayer is between $z = -5$ and $z = 0$; distances are in nm; and the permittivities are $\epsilon_w = \epsilon_c = 80\epsilon_0$ and $\epsilon_\ell = 2\epsilon_0$.

two layers of high-permittivity dielectric to represent the head groups of the phospholipids.
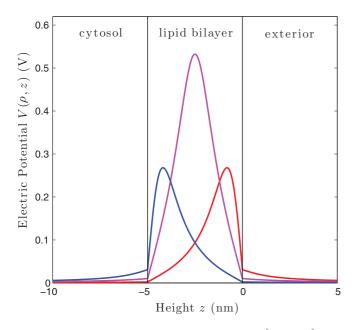

FIG. 2. (Color online) The electric potentials $V_w^\ell(\rho,z)$, $V_\ell^\ell(\rho,z)$, and $V_c^\ell(\rho,z)$ [(15), (16), and (17)] (V) for $\rho = 1$ as a function of the height z above the phospholipid bilayer for a unit charge $q = |e|$ in the phospholipid bilayer at $(\rho,z) = (0,-4.5)$ (left curve, blue), $(0,-2.5)$ (middle curve, magenta), and $(0,-0.5)$ (right curve, red). Distances and permittivities are as in Fig. 1.

III. A SURFACE CHARGE ON A MEMBRANE

As a pedagogical application of the formulas of the preceding section, let us consider a uniform charge density σ on the surface of a lipid bilayer of thickness t. To avoid minus signs, I put the charge density on the extracellular leaflet. After doing the computation, I'll translate the result to the case of PS on the cytosolic leaflet.

Maxwell's jump equation (2) tells us that the electric displacement D_w in the water differs by σ from its value D_ℓ in the lipid, which in turn is the same as its value D_c in the cytosol. So we have two equations $D_w = D_\ell + \sigma$ and $D_\ell = D_c$ for three unknowns. We can use the electrostatic potentials of Sec. II to resolve this ambiguity.

The electrostatic potential $V_w^w(\rho,z)$ due to a point charge at $(0,0,h)$, as given by (9), is equal to the electrostatic potential $V_w^w(0,z)$ due to a point charge at (ρ,h). Thus setting the height h in (9) equal to zero, and differentiating with respect to z, we find for the z component of the electric field at $(0,0,z)$ due to a charge q at $(\rho,0)$

$$E_z(0,z) = -\left.\frac{\partial}{\partial z}V_w^w(\rho,z)\right|_{h=0} \tag{24}$$

or

$$E_z(0,z) = \frac{q}{4\pi\epsilon_w}\left\{\frac{(1+p)z}{r^3}\right.$$
$$\left.-p'(1-p^2)\sum_{n=1}^{\infty}\frac{(pp')^{n-1}(z+2nt)}{[\rho^2+(z+2nt)^2]^{3/2}}\right\}, \tag{25}$$

in which $r = \sqrt{\rho^2 + z^2}$ and $z \geqslant 0$. Replacing the charge q by $\sigma\,2\pi\rho d\rho$ and integrating over ρ from $\rho = 0$ to $\rho = \infty$, we have

$$E_z(\sigma) = \frac{2\pi\sigma}{4\pi\epsilon_w}\left[1 + p - p'(1-p^2)\sum_{n=0}^{\infty}(pp')^n\right]. \tag{26}$$

The dependence upon the variables z and t has dropped out. Doing the sum and using the definitions (6) of p and p', we get

$$E_z(\sigma) = \frac{\sigma}{2\epsilon_w}\left[1 + p - p'(1-p^2)\frac{1}{1-pp'}\right]$$
$$= \frac{\sigma}{2\epsilon_w}\frac{(1+p)(1-p')}{1-pp'} = \frac{\sigma}{\epsilon_w + \epsilon_c}. \tag{27}$$

The field points in the $\hat{z}$ direction.

In the limiting case in which the electric permittivity of the extracellular medium is the same as that of the cytosol, $\epsilon_w = \epsilon_c$, the electric field is $E_w(\sigma) = \sigma/2\epsilon_w$.

We may apply similar reasoning to the formula (11) for the potential $V_c^w(\rho,z)$ in the cytosol due to a charge q in the extracellular water at a height h above the membrane. If we keep in mind that the quantity $z - 2nt - h$ is negative, then we find for the electric field in the cytosol of a surface-charge density σ at $h = 0$

$$E_c(\sigma) = -\frac{\sigma}{\epsilon_w + \epsilon_c}. \tag{28}$$

Since there is no surface charge between the cytosol and the membrane, it follows from Maxwell's jump equation (2) that

$D_\ell = \epsilon_\ell E_\ell = D_c = \epsilon_c E_c$, and so that the electric field in the membrane is proportional to that in the cytosol

$$E_\ell(\sigma) = \frac{\epsilon_c}{\epsilon_\ell} E_c(\sigma). \tag{29}$$

Our formula (28) for $E_c(\sigma)$ now gives $E_\ell(\sigma)$ as

$$E_\ell(\sigma) = -\frac{\sigma \epsilon_c}{\epsilon_\ell(\epsilon_w + \epsilon_c)}. \tag{30}$$

The jump in the displacement D across the layer of surface charge is

$$D_w - D_\ell = \frac{\sigma \epsilon_w}{(\epsilon_w + \epsilon_c)} + \frac{\sigma \epsilon_c}{\epsilon_w + \epsilon_c} = \sigma, \tag{31}$$

in agreement with Maxwell's equation (2).

If the layer of surface charge of density, like that of PS, lies on the cytosolic leaflet at $z = -t$, then the electric fields are

$$\begin{aligned} E_w(\sigma) &= \frac{\sigma}{\epsilon_w + \epsilon_c}, \\ E_\ell(\sigma) &= \frac{\sigma \epsilon_w}{\epsilon_\ell(\epsilon_w + \epsilon_c)}, \\ E_c(\sigma) &= -\frac{\sigma}{\epsilon_w + \epsilon_c}. \end{aligned} \tag{32}$$

IV. IMAGE CHARGES

As noted by Wagner [2], a charge q in or near a membrane polarizes the membrane and the surrounding water. The potential formulas (9)–(11), (15)–(17), and (21)–(23) represent these bound charges as infinitely many mirror charges. The mirror charges affect the behavior of ions near an interface between two dielectrics in ways that mean-field theories cannot describe.

For instance, a charge q in the lipid bilayer induces mirror charges in the cytosol and in the extracellular environment. These induced charges are of opposite sign, and they attract the charge q in the lipid membrane. We can be more precise about this attraction if in the formula (16) for $V_\ell^\ell(\rho,z)$, we use $V_\ell^\ell(z)$ to represent the self-potential $V_\ell^\ell(0,z)$ without the z independent, infinite, $n = 0$ term of the first sum

$$\begin{aligned} V_\ell^\ell(z) = \frac{q}{4\pi\epsilon_\ell} \Bigg[&-\frac{\ln(1 - p\, p')}{t} \\ &- \sum_{n=0}^{\infty} \frac{p\,(pp')^n}{|2z - 2nt|} - \frac{p'\,(pp')^n}{|2z + 2(n+1)t|} \Bigg]. \end{aligned} \tag{33}$$

Keeping only the first term in each sum and using C for the constant log term, we recognize two image charges

$$V_\ell^\ell(z) \approx \frac{q}{4\pi\epsilon_\ell} \left(C - \frac{p}{|2z|} - \frac{p'}{|2z + 2t|} \right) \tag{34}$$

familiar from freshman physics. They attract the charge q no matter what its sign. Water is better than lipid at attracting charges.

Similarly, a charge q in the extracellular water induces a mirror charge in the lipid and others in the cytosol. The mirror charge in the lipid is of the same sign and, being closer, repels the charge q. We can describe this repulsion in terms of the

formula (9) for $V_w^w(\rho,z)$ if we use $V_w^w(z)$ to mean $V_w^w(0,z)$ without the z-independent, infinite term $1/r$,

$$V_w^w(z) = \frac{q}{4\pi\epsilon_w} \left[\frac{p}{|2z|} - \frac{\epsilon_w \epsilon_\ell}{\epsilon_{w\ell}^2} \sum_{n=1}^{\infty} \frac{p^{n-1}p'^n}{|2z + 2nt|} \right]. \tag{35}$$

The first term is the potential of the textbook mirror charge

$$V_w^w(z) \approx \frac{q}{4\pi\epsilon_w} \frac{p}{|2z|}. \tag{36}$$

An ion of charge q in this potential has an energy proportional to $q^2 p$, which is positive for both cations and anions. A lipid membrane therefore repels both cations and anions; the water attracts the ion more than the lipid does. In a mean-field theory, such as unpatched Poisson-Boltzmann theory, every particle responds to the *same* potential $V(x)$, so the force $qE(x) = -q\nabla V(x)$ is proportional to the charge q of the ion and therefore must be *opposite* for cations and anions. Mean-field theories cannot describe why a lipid membrane repels *both* cations and anions.

V. IONS NEAR A CHARGED MEMBRANE

One can use the formulas of Sec. II in a Monte Carlo code to compute the distribution of salt ions near a charged membrane. Here I present the result of such a simulation of the distributions of potassium and chloride ions near a membrane of a vesicle whose inner leaflet contains PS at a level of 4%, which is about that of the plasma membrane of a liver cell.

In the simulation, I let the potassium and chloride ions move according to a Metropolis algorithm within a box whose width and length were 50 nm and whose height was 10 nm. I took the potassium concentration to be 150 mM so as to allow for a 10 mM concentration of sodium ions. The box contained 2258 K^+ ions. The bottom of the box was covered by a uniform negative surface charge density whose total charge was $-143\,|e|$ corresponding to 143 PSs at a molar density of 4%. I used 2115 Cl^- ions to make the whole system neutral; these chloride ions played the role of the whole ensemble of anionic cell constituents.

To mitigate edge effects, I surrounded the box with eight identical boxes into which I mirrored all 4373 ions. So there were 39 357 ions in nine identical boxes. All the boxes had the same uniform surface-charge density due to the presence of the PSs at a level of 4%. To strictly enforce periodic boundary conditions, one should use Ewald sums [10], but I did not do this because they would have slowed the code down and because liquids are not crystals. Since the maximum step size in the z direction was only 1 Å; the error due to using only eight boxes of mirrored ions altered the energy difference ΔE of a Monte Carlo move by less than $0.064kT$, usually about $0.016kT$, far less than the thermal noise.

In my Monte Carlo code [11], I used the constant (27) for the electric field $E_z(\sigma)$ of the surface charge of PSs, the series (35) for the self-potential $V_w^w(z)$ arising from the response of the bound charge to an ion of charge q, and the sum (9) for the electrostatic potential $V_w^w(\rho,z)$ due to a charge in the extracellular water near a membrane. In this way, I took exact account of the fields of the charges of the problem while treating the neutral molecules of the extracellular environment, the membrane, and the cytosol as bulk dielectric media. The

simulations consisted of eight separate runs in which 23 000 sweeps were allowed for thermalization. Four of the runs collected data for an additional 50 000 sweeps; the other four for an additional 9000 sweeps.

In Poisson-Boltzmann theory [12], all charges respond to a common potential V that obeys Poisson's equation with a charge density that respects the Boltzmann distribution

$$-\epsilon \, \triangle V = \rho_{pf} + \sum_i \rho_{f0i} \, e^{-q_i V/kT}. \tag{37}$$

Here V is the electrostatic potential, ρ_{pf} is a prescribed distribution of free charge, q_i is the charge of species i, and ρ_{f0i} is its free-charge density where V vanishes [12]. This nonlinear equation is hard to solve except in one-dimensional problems where the Gouy-Chapman solution [2] is available [12]. In the present context, that solution for the potential $V(z)$ is [12]

$$V(z) = -\frac{2kT}{e} \, \ln\left[\frac{1 + e^{-(z+z_0)/\lambda}}{1 - e^{-(z+z_0)/\lambda}}\right], \tag{38}$$

in which $\lambda = 1/\sqrt{8\pi \ell_B c_\infty}$, the Bjerrum length is $\ell_B = e^2/4\pi\epsilon_w kT$, and c_∞ is the bulk ion concentration (taken to be the same for potassium and chloride). If σ is half the absolute value of the surface-charge density of the PSs, then the offset is

$$z_0 = \lambda \ln \left\{\frac{e}{2\pi \ell_B \lambda \sigma} \left[1 + \sqrt{1 + (2\pi \ell_B \lambda \sigma)^2}\right]\right\}. \tag{39}$$

The Gouy-Chapman formulas for the concentrations of the potassium and chloride ions (normalized to unity where $V = 0$) are then

$$\mathrm{K_{GC}}(z) = e^{-eV(z)/kT} \quad \text{and} \quad \mathrm{Cl_{GC}}(z) = e^{eV(z)/kT}. \tag{40}$$

In Fig. 3, I have plotted my Monte Carlo predictions for the relative concentrations of potassium ions $\rho_K(z)/\bar{\rho}_K$ (red solid curve) and of chloride ions $\rho_{Cl}(z)/\bar{\rho}_{Cl}$ (blue dashed curve) as functions of the distance z from the charged membrane. The Gouy-Chapman predictions (40) for the normalized potassium $\mathrm{K_{GC}}(z)$ (red, dot-dash) and chloride $\mathrm{Cl_{GC}}(z)$ (blue, dots) concentrations also are plotted there. The solid $\mathrm{K^+}$ and dashed $\mathrm{Cl^-}$ Monte Carlo concentrations correctly drop sharply for, respectively, $z < 1$ and $z < 2$ nm due to the repulsion by the induced image charges as discussed in Sec. IV. These concentrations are much lower than the Gouy-Chapman predictions. The Gouy-Chapman-Poisson-Boltzmann potassium concentration actually rises monotonically when the $\mathrm{K^+}$ is less than 4 nm from the membrane. [The behavior of both $\rho_K(z)/\bar{\rho}_K$ and $\rho_{Cl}(z)/\bar{\rho}_{Cl}$ for $z > 9$ nm is an artifact due to the absence of ions at $z > 10$ nm in the simulation.]

In Fig. 4, I have plotted my Monte Carlo predictions for the average total potential that a $\mathrm{K^+}$ ion (solid, red) or a $\mathrm{Cl^-}$ ion (dashed, blue) feels due to the surface charge of the PSs, to the other ions, and to its polarization of the three dielectrics. The induced bound charge sharply raises the potential felt by the potassium ion for $z < 1$ nm and lowers that felt by a chloride ion for $z < 2$ nm. The dot-dash magenta curve represents the potential due to the surface-charge layer of PSs and to all the ions (including the bound charges they induce) but without the image charges of Eq. (35). These three potentials differ significantly over the whole range in which the Gouy-Chapman concentrations differ from their bulk values. (The
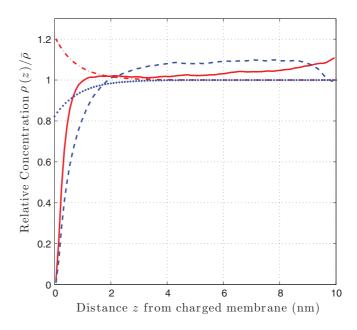

FIG. 3. (Color online) Monte Carlo predictions for the relative concentrations of potassium $\rho_K(z)/\bar{\rho}_K$ (solid, red) and chloride $\rho_{Cl}(z)/\bar{\rho}_{Cl}$ (dashed, blue) ions at a distance z (nm) from the charged cytosolic leaflet of a lipid bilayer are plotted along with the Gouy-Chapman predictions (40) for the normalized potassium $\mathrm{K_{GC}}(z)$ (dot-dash, red) and chloride $\mathrm{Cl_{GC}}(z)$ (dots, blue) concentrations.

dip in the three potentials for $z > 9$ nm is an artifact due to the absence of ions at $z > 10$ nm.)

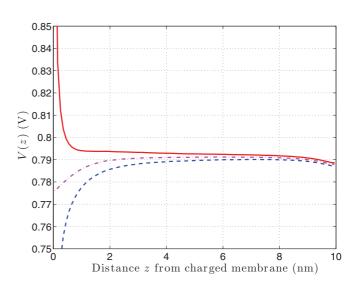In the related papers [9,13], I neglected the self-potential.

FIG. 4. (Color online) Monte Carlo predictions for the average total electrostatic potential $V(z)$ (V) at a distance z (nm) from the charged cytosolic leaflet of a lipid bilayer as felt by a $\mathrm{K^+}$ (solid, red) and by a $\mathrm{Cl^-}$ (dashed, blue) ion. The potential is that due to the PSs of the cytosolic leaflet, the ions of the cytosol, and the polarization induced by the $\mathrm{K^+}$ ion or by the $\mathrm{Cl^-}$ ion. The dot-dash magenta curve is the average potential felt by the ion without the self-potential (35) that represents the polarization the ion induces.

VI. VALIDITY OF THE DEBYE LAYER

We have seen in the last two sections that mean-field theory cannot account for the behavior of ions near an interface between two dielectrics with two very different permittivities. Does this mean that the usual interpretation of the Debye layer is incorrect?

The answer depends upon the difference between the two permittivities and upon the magnitude of the surface-charge density. An image charge is proportional to the ratio of the difference of the two permittivities to their sum. So if the dielectrics have similar permittivities, then the induced charges will be weak, and the image-charge correction to a mean-field Debye layer will be small. Similarly, a high surface-charge density will dominate the field due to the induced bound charges unless the ions are very close to the interface. Thus the validity of the Debye layer depends on the relative magnitudes of the self-potential $V_w^w(z) \approx qp/8\pi\epsilon_w|z|$ due to the image-charge correction (35) and the potential $V_\sigma(z) = -\sigma |z|/(\epsilon_w + \epsilon_c)$ due to the electric field (32) of the PSs. In Fig. 5, I have plotted for a K$^+$ ion both their sum $V_w^w(z) + V_\sigma(z)$ and the potential $V_\sigma(z)$. For the surface-charge density σ of a 4 mol % concentration of PS, as on the cytosolic leaflet of a liver cell, the sum $V_w^w(z) + V_\sigma(z)$ (red solid curve) differs from the surface-charge potential $V_\sigma(z)$ (red dashed straight line) for $z < 2$ nm. However, for a higher mole percent of 20%, the relative difference between the sum $V_w^w(z) + V_\sigma(z)$ (blue dot-long-dash curve) and $V_\sigma(z)$ (blue dotted straight line) is somewhat less.

The importance of the image-charge correction (35) rises as the surface-charge density falls. It is therefore particularly
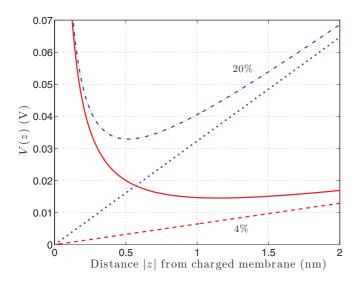

FIG. 5. (Color online) For a potassium ion, the sum $V_w^w(z) + V_\sigma(z)$ of the electrostatic potential $V_w^w(z)$ due to the induced mirror charges (35) and that $V_\sigma(z) = -\sigma |z|/(\epsilon_w + \epsilon_c)$ due to the electric field (32) of a lipid bilayer whose cytosolic leaflet is charged to a PS mole percent of 4% (red, solid curve) or 20% (blue, dot-long-dash curve) is plotted against the distance $|z|$ (nm) from the leaflet. The uncorrected linear potentials $V_\sigma(z)$ of the two surface-charge densities, 4% (blue dots) and 20% (red dashes), appear as straight lines.

important in the case of an uncharged membrane, such as the outer leaflet of the plasma membrane.

VII. A ZWITTERION

Let us consider a simple model of a zwitterionic molecule in salty water above an uncharged lipid bilayer. The toy zwitterion is just a point charge q' at r' and another q'' at r''. The charges are separated by $s = r' - r''$, which makes an angle θ with the vertical $\hat{z}$ so that $\hat{z} \cdot s = s \cos\theta$, where s is the distance between the charges $s = \sqrt{s^2}$. The square of the horizontal distance between the charges is $\rho^2 = (x' - x'')^2 + (y' - y'')^2 = s^2 \sin^2\theta$. The midpoint of the molecule is $r = (r' + r'')/2$ and its mean height is $z = \hat{z} \cdot r$. The heights of the charges are $z' = z + \frac{1}{2}s\cos\theta$ and $z'' = z - \frac{1}{2}s\cos\theta$.

The electrostatic energy $E'(z')$ of the interaction of the point charge q' with the polarization it induces is $E'(z') = q'^2 u(z') = q'^2 u(z + \frac{1}{2}s\cos\theta)$ in which $u(z)$ is the infinite sum (35) of image charges

$$u(z) = \frac{1}{4\pi\epsilon_w}\left[\frac{p}{|2z|} - \frac{\epsilon_w\epsilon_\ell}{\epsilon_{w\ell}^2}\sum_{n=1}^{\infty}\frac{p^{n-1}p'^n}{|2z + 2nt|}\right]. \quad (41)$$

Similarly, the function $u(z)$ gives the energy of the interaction of the other point charge q'' with the polarization it induces as $E''(z'') = q''^2 u(z'') = q''^2 u(z - \frac{1}{2}s\cos\theta)$.

To find the energy $E(r',r'')$ of the charge q' in the full potential of the charge q'' and the energy $E(r'',r')$ of the charge q'' in the full potential of the charge q', we use our formula (9) for the potential $V_w^w(\rho,z)$. To compute $E(r',r'')$, we imagine the charge q'' to be at $(x'',y'',z'') = (0,0,h)$ and the charge q' to be at $(\rho,z,0)$ in cylindrical coordinates. Then $E(r',r'')$ is $q'q''V_w^w(\rho,z)/q$, where

$$\frac{V_w^w(\rho,z)}{q} = \frac{1}{4\pi\epsilon_w}\left[\frac{1}{s} + \frac{p}{\sqrt{\rho^2 + (z' + z'')^2}}\right.$$
$$\left. - p'(1 - p^2)\sum_{n=1}^{\infty}\frac{(pp')^{n-1}}{\sqrt{\rho^2 + (z' + 2nt + z'')^2}}\right]. \quad (42)$$

This interaction is unchanged when we interchange the locations of the two charges, and $z' + z'' = 2z$. So $E(r',r'') = E(r'',r') = q'q''v(z,\theta,s)$, where

$$v(z,\theta,s) = \frac{1}{4\pi\epsilon_w}\left[\frac{1}{s} + \frac{p}{\sqrt{s^2 \sin^2\theta + (2z)^2}}\right.$$
$$\left. - p'(1 - p^2)\sum_{n=1}^{\infty}\frac{(pp')^{n-1}}{\sqrt{s^2\sin^2\theta + (2z + 2nt)^2}}\right]. \quad (43)$$

The total electrostatic energy of the molecule is then

$$E(z,\theta) = q'^2 u(z + \tfrac{1}{2}s\cos\theta) + q''^2 u(z - \tfrac{1}{2}s\cos\theta)$$
$$+ 2q'q''v(z,\theta,s). \quad (44)$$

In Fig. 6, I plot the energy (44) of the model zwitterion when it is z nm away from a plasma membrane considered as a lipid slab with salty water on both sides. The four lower, solid curves are for a point charge $q' = |e|$ separated by 0.5 nm
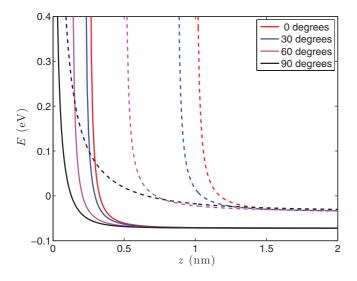
FIG. 6. (Color online) The energy (44) of a zwitterion in salty water a distance z from a lipid slab. The four lower, solid curves are for a molecule consisting of a point charge $q' = |e|$ separated by 0.5 nm from a charge $q'' = -|e|$; the four upper, dashed curves are for a molecule consisting of a point charge $q' = 2|e|$ separated by 2 nm from a charge $q'' = -|e|$. Within each quartet the molecules from right to left make angles of $0°$, $30°$, $60°$, and $90°$ with the vertical.

from a charge $q'' = -|e|$; the four upper, dashed curves are for a point charge $q' = 2|e|$ separated by 2 nm from a charge $q'' = -|e|$. The lipid slab repels the molecules.

One may find the energy of a more realistic zwitterion by integrating the two-charge formula (44) over a suitable charge distribution.

VIII. SEVERAL DIELECTRIC LAYERS

We may extend our derivation of the electric potential of a charge in a material of three dielectrics to the case of several dielectrics. One biological application is to a phospholipid bilayer considered as a layer of lipids bounded by two thin layers of head groups. These three layers with the extracellular water and the cytosol pose a five-dielectric problem.

Let us first consider the case of four dielectric layers with the charge q in the first layer of permittivity ϵ_w in the region $z > 0$. Instead of the three potentials (4), we have four

$$V_w^w(\rho,z) = \int_0^\infty dk\, J_0(k\rho) \left[\frac{q}{4\pi\epsilon_w} e^{-k|z-h|} + u(k)\, e^{-kz} \right],$$

$$V_1^w(\rho,z) = \int_0^\infty dk\, J_0(k\rho)[m_1(k)\, e^{kz} + f_1(k)\, e^{-kz}],$$

$$V_2^w(\rho,z) = \int_0^\infty dk\, J_0(k\rho)[m_2(k)\, e^{kz} + f_2(k)\, e^{-kz}],$$

$$V_c^w(\rho,z) = \int_0^\infty dk\, J_0(k\rho)\, d(k)\, e^{kz}, \quad (45)$$

in which the first internal layer of permittivity ϵ_1 fills the region $-t_1 < z < 0$ while the second internal layer of permittivity ϵ_2 fills the region $-t_1 - t_2 < z < -t_1$. The constraints (1) and (2) give six equations,

$$m_1 + f_1 - u = \beta,$$

$$\epsilon_1 m_1 - \epsilon_1 f_1 + \epsilon_w u = \epsilon_w \beta,$$

$$m_1 + y_1 f_1 - m_2 - y_1 f_2 = 0,$$

$$\epsilon_1 m_1 - \epsilon_1 y_1 f_1 - \epsilon_2 m_2 + \epsilon_2 y_1 f_2 = 0,$$

$$m_2 + y_2 f_2 - d = 0,$$

$$\epsilon_2 m_2 - \epsilon_2 y_2 f_2 - \epsilon_c d = 0, \quad (46)$$

in which $y_1(k) = \exp(2kt_1)$ and $y_2(k) = \exp[2k(t_1 + t_2)]$, while as in (5) the parameter $\beta(k) = q \exp(-kh)/4\pi\epsilon_w$ represents the charge at $z = h > 0$. The functions $m_1(k)$ and $f_1(k)$ determine $m_2(k)$ and $f_2(k)$ as

$$m_2 = [(\epsilon_2 + \epsilon_1)m_1 + (\epsilon_2 - \epsilon_1)y_1 f_1]/2\epsilon_2,$$

$$f_2 = [(\epsilon_2 - \epsilon_1)m_1/y_1 + (\epsilon_2 + \epsilon_1)f_1]/2\epsilon_2. \quad (47)$$

We now address the problem of a charge q in a semi-infinite region of permittivity ϵ_w at a height h above n internal layers of permittivity ϵ_i and thickness t_i, which in turn are above a semi-infinite region of permittivity ϵ_c. In the ith internal layer, the potential is

$$V_i^w(\rho,z) = \int_0^\infty dk\, J_0(k\rho)[m_i(k)\, e^{kz} + f_i(k)\, e^{-kz}], \quad (48)$$

while the first and fourth equations of the set (45) describe the potentials in the two semi-infinite regions. The functions $m_i(k)$ and $f_i(k)$ determine those $m_{i+1}(k)$ and $f_{i+1}(k)$ of the next layer by matrix multiplication. If

$$p_i = \frac{\epsilon_{i+1} - \epsilon_i}{\epsilon_{i+1} + \epsilon_i} \quad \text{and} \quad \overline{\epsilon}_i = \frac{\epsilon_{i+1} + \epsilon_i}{2}, \quad (49)$$

then

$$\begin{pmatrix} m_{i+1} \\ f_{i+1} \end{pmatrix} = \frac{1}{2\epsilon_{i+1}} \begin{pmatrix} \epsilon_{i+1} + \epsilon_i & (\epsilon_{i+1} - \epsilon_i)y_i \\ (\epsilon_{i+1} - \epsilon_i)/y_i & \epsilon_{i+1} + \epsilon_i \end{pmatrix} \begin{pmatrix} m_i \\ f_i \end{pmatrix}$$

$$= \frac{\overline{\epsilon}_i}{\epsilon_{i+1}} \begin{pmatrix} 1 & p_i y_i \\ p_i/y_i & 1 \end{pmatrix} \begin{pmatrix} m_i \\ f_i \end{pmatrix}, \quad (50)$$

in which $y_0 = 1$ and $y_i = \exp[2k(t_1 + \cdots + t_i)]$ for $i > 0$. Let us set $m_0(k) = \beta(k)$ and $f_0(k) = u(k)$ as well as $m_{n+1}(k) = d(k)$ and $f_{n+1}(k) = 0$. In these formulas, ϵ_{n+1} is ϵ_c, and ϵ_0 is ϵ_w, not the permittivity of the vacuum. If E_ℓ is the product of $\ell + 1$ of the matrices (50)

$$E^{(\ell)} = \prod_{i=0}^{\ell} \frac{\overline{\epsilon}_i}{\epsilon_{i+1}} \begin{pmatrix} 1 & p_i y_i \\ p_i/y_i & 1 \end{pmatrix}, \quad (51)$$

then we have

$$\begin{pmatrix} m_{i+1} \\ f_{i+1} \end{pmatrix} = E^{(i)} \begin{pmatrix} \beta \\ u \end{pmatrix}. \quad (52)$$

Setting $i = n$ gives us

$$u = -\beta\, E_{21}^{(n)}/E_{22}^{(n)},$$

$$d = \beta \left(E_{11}^{(n)} - E_{12}^{(n)} E_{21}^{(n)}/E_{22}^{(n)} \right). \quad (53)$$

IX. THREE DIELECTRIC LAYERS

A phospholipid bilayer consists of a layer of phosphate head groups, a (double) layer of lipids, and a second layer of phosphate head groups. In this section, we apply the formulas of Sec. VIII to the problem of a charge q at a height h above

such a bilayer. There are now three slabs and two semi-infinite regions. We must compute $E^{(3)}$. I get

$$E_{21}^{(3)} = p_0 + \frac{p_1}{y_1} + \frac{p_2}{y_2} + \frac{p_0 p_1 p_2 y_1}{y_2}$$
$$+ \frac{p_3}{y_3}\left(1 + p_0 p_1 y_1 + p_0 p_2 y_2 + \frac{p_1 p_2 y_2}{y_1}\right) \quad (54)$$

and

$$E_{22}^{(3)} = 1 + \frac{p_0 p_1}{y_1} + \frac{p_0 p_2}{y_2} + \frac{p_1 p_2 y_1}{y_2}$$
$$+ \frac{p_3}{y_3}\left(p_0 + p_1 y_1 + p_2 y_2 + \frac{p_0 p_1 p_2 y_2}{y_1}\right). \quad (55)$$

Stern and Feller [14], Nymeyer and Zhou [15], and Baker [16] have estimated the relative electric permittivity of phospholipid membranes as being 1 from 0 to 10 Å from the center, 4 from 10 to 15 Å, 180 from 15 to 20 Å, 210 from 20 to 25 Å, and like bulk water beyond 25 Å. I approximate their results by using 2 from 0 to 15 Å and 195 from 15 to 25 Å and take the relative permittivities of the cytosol and of the extracellular environment to be 80. These approximations greatly simplify our formulas (54) and (55) and imply that $p_0 = 0.418 = -p_3$ and $p_1 = -0.98 = -p_2$. The thicknesses of the layers are $t_1 = t \equiv 1$ nm, $t_2 = 3t$, and $t_3 = t$, and so $y_1 = e^{2kt}$, $y_2 = e^{8kt}$, and $y_3 = e^{10kt}$. With these simplifications, our formulas (54) and (55) reduce to

$$E_{21}^{(3)} = p_0 + p_1(e^{-2kt} - e^{-8kt}) - p_0 p_1^2 e^{-6kt}$$
$$- p_0 e^{-10kt}\left(1 + p_0 p_1(e^{2kt} - e^{8kt}) - p_1^2 e^{6kt}\right)$$
$$= p_0 + p_0 p_1^2 e^{-4kt} + p_1(1 + p_0^2)(e^{-2kt} - e^{-8kt})$$
$$- p_0 e^{-10kt} - p_0 p_1^2 e^{-6kt} \quad (56)$$

and

$$E_{22}^{(3)} = 1 + p_0 p_1(e^{-2kt} - e^{-8kt}) - p_1^2 e^{-6kt}$$
$$- p_0 e^{-10kt}\left(p_0 + p_1(e^{2kt} - e^{8kt}) - p_0 p_1^2 e^{6kt}\right)$$
$$= 1 + p_0^2 p_1^2 e^{-4kt} + 2p_0 p_1(e^{-2kt} - e^{-8kt})$$
$$- p_0^2 e^{-10kt} - p_1^2 e^{-6kt}. \quad (57)$$

The key function $u(k)$ then is by (53) the ratio

$$u(k) = -\frac{q}{4\pi\epsilon_w} e^{-kh}\big[p_0 + p_1(1 + p_0^2)(e^{-2kt} - e^{-8kt})$$
$$+ p_0 p_1^2 e^{-4kt} - p_0 p_1^2 e^{-6kt} - p_0 e^{-10kt}\big]$$
$$\big/\big[1 + 2p_0 p_1(e^{-2kt} - e^{-8kt}) + p_0^2 p_1^2 e^{-4kt}$$
$$- p_1^2 e^{-6kt} - p_0^2 e^{-10kt}\big]. \quad (58)$$

We can use it and our formula (45) to write the potential $V_w^w(\rho, z)$ at the point (ρ, z) due to a charge q on the z axis at $(0, h)$ above a three-slab phospholipid bilayer as

$$V_w^w(\rho, z) = \int_0^\infty dk\, J_0(k\rho)\left[\frac{q}{4\pi\epsilon_w} e^{-k|z-h|} + u(k)\,e^{-kz}\right]. \quad (59)$$

Figure 7 plots this potential $V_w^w(\rho, z)$ for $\rho = 1$ nm and $0 \leqslant z \leqslant 5$ nm for the case of a unit positive charge $q = |e|$ on
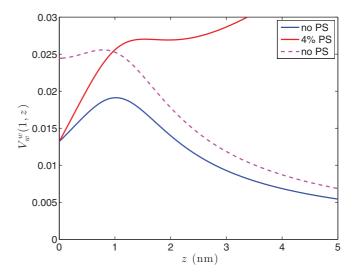

FIG. 7. (Color online) The potential $V_w^w(\rho, z)$ [V, (59)] at the point (ρ, z) due to a charge $q = |e|$ on the z axis at $(0, h)$ above a three-slab phospholipid bilayer that is neutral (lowest, solid, blue) or has a 4 mol % layer of PS on its cytosolic leaflet (upper, solid, red). Both ρ and h are 1 nm. The potential (9) of a charge above a single neutral lipid slab without head groups is plotted as a dashed magenta curve to illustrate the effect of the layers of head groups.

the z axis at height $h = 1$ nm above a three-slab phospholipid bilayer that is neutral (lowest curve, solid, blue) or has a 4 mol % layer of PS on its cytosolic leaflet (upper curve, solid, red). The electric field of the PSs is taken from (32) to be $E_w(\sigma) = \sigma/(\epsilon_w + \epsilon_c)$ in which σ is negative. To illustrate the effect of the layers of head groups with very high electric permittivity, I have replotted the potential (9) of Fig. 1 due to the same charge but above a single naked, neutral lipid slab as a dashed magenta curve. The head-group dipoles lower the potential $V_w^w(\rho, z)$ in their vicinity.

We also can use the ratio $u(k)$ to compute the self-interaction of a charge q with our three slab model of the phospholipid bilayer. The potential felt by the charge in the salty water due to all the image charges its presence induces in the three slabs and in the cytosol is

$$V_w^w(z) = \int_0^\infty u(k)\,e^{-kz}\,dk, \quad (60)$$

in which $u(k)$ is the ratio (58) but with the height h of the charge q replaced with z. The potential felt by the charge q at z then is

$$V_w^w(z) = -\frac{q}{4\pi\epsilon_w t}\int_0^\infty e^{-2kz/t}\big[p_0 + p_0 p_1^2 e^{-4k} - p_0 e^{-10k}$$
$$+ p_1(1 + p_0^2)(e^{-2k} - e^{-8k}) - p_0 p_1^2 e^{-6k}\big]$$
$$\big/\big[1 + p_0^2 p_1^2 e^{-4k} - p_0^2 e^{-10k}$$
$$+ 2p_0 p_1(e^{-2k} - e^{-8k}) - p_1^2 e^{-6k}\big]\,dk, \quad (61)$$

in which the parameter t is 1 nm.

Figure 8 plots the electric potential felt by an ion of charge $|e|$ near a phospholipid bilayer modeled as a lipid slab bounded by two thin polar slabs. The lowest (solid, blue) curve is for a neutral membrane; the upper (solid, red) curve is for
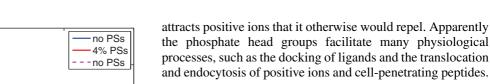
FIG. 8. (Color online) The potential $V_w^w(z)$ [V, (61)] felt by a unit positive charge at a height z nm above a phospholipid membrane modeled as a lipid slab bounded by two thin polar slabs. The lowest (solid, blue) curve is for a neutral membrane; the upper (solid, red) curve is for a membrane whose cytosolic leaflet is negatively charged by PS at 4 mol %. Without the outer polar slabs, the potential (35) is purely repulsive (dashed magenta).

a membrane whose cytosolic leaflet is negatively charged by PS at 4 mol % represented as in Fig. 7. The two thin layers of phosphate head groups make the potential felt by an ion near a neutral phospholipid bilayer attractive rather than repulsive. Without the outer polar slabs, the potential (35) is purely repulsive (dashed magenta). The head groups attract to the membrane ions that a naked lipid slab would repel. If the membrane has PSs on its cytosolic leaflet, then it strongly

attracts positive ions that it otherwise would repel. Apparently the phosphate head groups facilitate many physiological processes, such as the docking of ligands and the translocation and endocytosis of positive ions and cell-penetrating peptides.

X. SUMMARY

I derived the electrostatic potential of a charge in or near a lipid bilayer in Sec. II and used it in Sec. III to compute the electric field of a uniformly charged membrane and in Sec. IV to describe the effects of image charges. In Sec. V, I used the results of Sec. II–IV in a Monte Carlo computation of the distribution of ions near a charged membrane. I discussed the validity of the Debye layer in Sec. VI and computed the energy of a zwitterion near a lipid slab in Sec. VII. In Sec. VIII, I calculated the potential of a charge near a membrane modeled as several dielectric layers of different permittivities between two different semi-infinite dielectrics. I used this analysis in Sec. IX to model a phospholipid bilayer as a lipid layer bounded by two layers of head groups of high electric permittivity. The phosphate head groups cause a neutral membrane to attract rather than to repel ions.

[1] E. M. Bevers, P. Comfurius, D. W. Dekkers, and R. F. Zwaal, Biochim. Biophys. Acta **1439**, 317 (1999); B. Alberts, A. Johnson, J. Lewis, M. Raff, K. Roberts, and P. Walter, *Molecular Biology of the Cell*, 4th ed. (Garland Science, New York, 2002), pp. 587–593.

[2] G. L. Gouy, J. Phys. **9**, 457 (1910); D. L. Chapman, Philos. Mag. Ser. 6, **25**, 475 (1913); C. Wagner, Phys. Zeits. **25**, 474 (1924).

[3] L. Onsager and N. N. T. Samaras, J. Chem. Phys. **2**, 528 (1934).

[4] A. Parsegian, Nature (London) **221**, 844 (1969); D. Walz, E. Bamberg, and P. Läuger, Biophys. J. **9**, 1150 (1969); B. Neumcke and P. Läuger, *ibid*. **9**, 1160 (1969); B. Neumcke, D. Walz, and P. Läuger, *ibid*. **10**, 172 (1970); R. H. Brown, Prog. Biophys. Mol. Biol. **28**, 341 (1974); A. Parsegian, Ann. N.Y. Acad. Sci. **264**, 161 (1975); B. Jönsson, H. Wennerström, and B. Halle, J. Phys. Chem. **84**, 2179 (1980); S. McLaughlin, Annu. Rev. Biophys. Biophys. Chem. **18**, 113 (1989); R. R. Netz, Eur. Phys. J. E **3**, 131 (2000); Y. Levin and J. E. Flores-Mena, Europhys. Lett. **56**, 187 (2001); R. Allen and J.-P. Hansen, Mol. Phys. **101**, 1575 (2003); Y. Levin, Europhys. Lett. **76**, 163 (2006); Y. S. Jho, G. G. Park, C. S. Chang, P. A. Pincus, and M. W. Kim, Phys. Rev. E **76**, 011920 (2007); A. P. Shreve, M. C. Howland, A. R. Sapuri-Butti, T. W. Allen, and A. N. Parikh, Langmuir **24**, 13250 (2008); D. Frydel, J. Chem.

Phys. **134**, 234704 (2011); N. Shimokawa, S. Komura, and D. Andelman, Phys. Rev. E **84**, 031919 (2011).

[5] A. Bakhshandeh, A. P. dos Santos, and Y. Levin, Phys. Rev. Lett. **107**, 107801 (2011).

[6] G. V. Miloshevsky, A. Hassanein, M. B. Partenskii, and P. C. Jordan, J. Chem. Phys. **132**, 234707 (2010).

[7] M. A. Wilson and A. Pohorille, JACS **118**, 6580 (1996); S. Dorairaj and T. W. Allen, Proc. Natl. Acad. Sci. USA **104**, 4943 (2007).

[8] J. Schwinger, L. Deraad, K. A. Milton, and W.-y. Tsai, *Classical Electrodynamics* (Westview Press, Boulder, CO, 1998), Chap. 16.

[9] K. E. Cahill, Phys. Biol. **7**, 016001 (2010).

[10] P. P. Ewald, Ann. Phys. **369**, 253 (1921).

[11] K. E. Cahill, FORTRAN-90 codes for the Monte Carlo simulations of this paper (2011), [http://bio.phys.unm.edu/~kevin/membraneElectrostatics/index.html].

[12] P. Nelson, *Biological Physics*, updated 1st ed. (Freeman, New York, 2008).

[13] K. E. Cahill, IET Syst. Biol. **4**, 367 (2010).

[14] H. A. Stern and S. E. Feller, J. Chem. Phys. **118**, 3401 (2003).

[15] H. Nymeyer and H.-X. Zhou, Biophys. J. **94**, 1185 (2008).

[16] N. Baker (private communication).